

Original article

# The metabolism of CYP2C9 and CYP2C19 for gliclazide by homology modeling and docking study

Yuan Yao <sup>a</sup>, Wei-Wei Han <sup>a</sup>, Yi-Han Zhou <sup>a</sup>, Ze-Sheng Li <sup>a,\*</sup>, Qiang Li <sup>b</sup>,  
Xiao-Yan Chen <sup>b</sup>, Da-Fang Zhong <sup>b,\*\*</sup>

<sup>a</sup> Institute of Theoretical Chemistry, State Key Laboratory of Theoretical and Computational Chemistry, Jilin University, Changchun 130023, PR China

<sup>b</sup> Center for Drug Metabolism Research, Shanghai Institute of Materia Medica, Chinese Academy of Sciences, Shanghai 201203, China

Received 30 September 2007; received in revised form 15 April 2008; accepted 23 April 2008

Available online 2 May 2008

## Abstract

With homology modeling techniques, a 3D structure model of CYP2C19 was built and refined with molecular mechanics and molecular dynamics simulations. The refined model was assessed to be reasonable by Profile-3D and PROCHECK programs. With the aid of the automatic molecular docking, one substrate and two inhibitors were docked to CYP2C19 by InsightII/Affinity program. The docking results, which are in well agreement with the reported results, demonstrate that the refined model of CYP2C19 is reliable. Then, with the refined model of CYP2C19 and the crystal structure of CYP2C9, the metabolisms of them for gliclazide in two different metabolic pathways were studied and the results show that both enzymes have more favorable interaction energies and stronger affinity with gliclazide in methylhydroxylation pathway than in 6 $\beta$ -hydroxylation pathway. It is exciting that substrate inhibition phenomenon can be found in metabolisms of CYP2C9 and CYP2C19 for gliclazide in two metabolic pathways. Gliclazide can change the conformation of the active sites and decrease obviously the affinities between gliclazide in the active site and enzymes when it is docked in the second active sites in CYP2C9 and CYP2C19. These results are in well agreement with the kinetic experimental results.

© 2008 Elsevier Masson SAS. All rights reserved.

**Keywords:** Cytochrome P450 protein; Gliclazide; Molecular docking; Substrate inhibition

## 1. Introduction

Diabetes is characterized by disrupted insulin production and sensitivity, leading to high blood glucose and a series of complications, for example, renal dysfunction, neuropathy and cardiopathy [1–4]. Type 2 diabetes mellitus, as a progressive, chronic disease, is characterized by insulin resistance, causing a decrease in transport of glucose into fat and muscle cells, and by a decrease in insulin secretion from the pancreas [5,6]. The most frequently used initial pharmacological agent is metformin. Metformin works as an insulin sensitizer,

predominantly by reducing glucose production from the liver [7], but its monotherapy often fails to maintain suitable glucose control for the long term [8]. Therefore, metformin with more than one agent, such as sulfonylurea, is used to keep successful control during the progressive course of the disease [9]. Gliclazide, 1-(4-methylbenzenesulfonyl)3-(3-azabicyclo[3.3.0]octyl)urea, is a second-generation sulfonylurea which is widely used in the treatment of type 2 diabetes as oral hypoglycaemic agent [10,11]. It is reported that gliclazide has similar efficacy to other sulfonylureas but has a lower risk of hypoglycaemia [12,13]. Gliclazide is extensively metabolized in humans, with only minor level of the unchanged drug detected in the urine samples. Two principal observed metabolites, resulting from oxidation of the methyl group, were methylhydroxygliclazide and carboxygliclazide, representing >30% of the urinary drug-related products.

\* Corresponding author. Tel.: +86 431 88498960; fax: +86 431 88498026.

\*\* Corresponding author. Tel./fax: +86 21 50800738.

E-mail addresses: [zeshengli@mail.jlu.edu.cn](mailto:zeshengli@mail.jlu.edu.cn) (Z.-S. Li), [zhongdf@china.com](mailto:zhongdf@china.com) (D.-F. Zhong).

Oxidation of the azabicyclooctyl ring was also confirmed with 6 $\beta$ -hydroxyglyclazide being the major representing 11% of the urinary products [14,15]. The two major metabolic pathways of glyclazide are listed in Fig. 1.

Park et al. suggested that glyclazide may be metabolized by CYP2C9 [16]. Zhang et al. reported that the pharmacokinetics of glyclazide MR is affected mainly by CYP2C19 genetic polymorphisms [17]. However, no detailed study has been performed to identify P450s involved in the hydroxylation of glyclazide. In this paper, homology modeling and automated molecular docking were performed to investigate metabolism of CYP2C9 and CYP2C19 for glyclazide.

## 2. Theory and methods

All simulations were performed on the SGI O3800 workstation using InsightII software package developed by Accelrys [18].

### 2.1. 3D model building of CYP2C19

The homology module [19] was used to build the initial model of CYP2C19 with the crystal structure of CYP2C9 (PDB code: 1R9O) [20] as the template. There are 92% amino acid sequence identity and 96% sequence similarity between CYP2C9 and CYP2C19 [21]. After 300 steps of conjugate gradient (CG) minimization, molecular dynamics (MD) simulation was performed to examine the quality of the model structure via 800 ps with the step size of 1 fs at a constant temperature 298 K. An explicit solvent model TIP3P water was used, and the homology solvent model was constructed with a 20 Å water cap from the center of mass of CYP2C19. Finally, a conjugate gradient energy minimization of full protein was performed until the root-mean-square (RMS) gradient energy was lower than 0.001 kcal mol/Å. All simulations mentioned above were accomplished without any constraint

under the consistent-valence force field (CVFF) by Discover3 software package [22]. The active site of CYP2C19 was not given any special treatment during homology modeling and molecular dynamic simulations. The optimized structure was checked by Profile-3D module [23] and PROCHECK program [24], respectively, to identify the reliability.

### 2.2. Flexible docking

Affinity [25], which uses a combination of Monte Carlo type and Simulated Annealing (SA) methods, is a suite of programs for automatically docking a ligand to a receptor in InsightII software package. A key feature is that the “bulk” of the receptor, defined as atoms not in the binding site specified, keeps rigid during the docking process, while the binding site atoms and ligand atoms are movable. By means of the 3D structures of the ligands which were built and optimized through the InsightII/Builder program, the automated molecular docking was performed by using docking program Affinity. The potential function of the complexes was assigned by using the consistent-valence force field (CVFF) and non-bonding interaction was dealt with the cell multipole approach. To account the solvent effect, the centered enzyme–ligand complexes were solvated in a sphere of TIP3P water molecules with radius 10 Å. The whole complex structure is further refined by energy minimization with 1000 steps. This provides 10 structures from SA docking and their generated conformations are clustered according to RMS deviation. The global structure with lowest energy is chosen for computing intermolecular binding energies. The docked complex of the receptor with the ligand is selected by the criteria of interacting energy combined with the geometrical matching quality and Ludi score. In general a higher Ludi score represents a higher affinity and stronger binding of a ligand to the receptor. Thus, for the complex structure, the Ludi program is used to character the affinity and the binding preference of a ligand to the receptor.

## 3. Results and discussion

The cytochrome P450 proteins represent a superfamily of heme-containing oxidative enzymes which are responsible for the metabolism of a structurally diverse range of drugs [26]. Heme can activate molecular oxygen and yielding water and an activated iron-oxygen species, which reacts with substrates through a variety of mechanisms [27]. As two major isoforms, CYP2C9 and CYP2C19 are highly conserved and exhibit 92% amino acid sequence identity and 96% sequence similarity [21]. Although only 43 of 490 amino acids differ between CYP2C9 and CYP2C19, they have different substrate selectivity and/or different regio-selectivity for some common substrates [28]. The crystal structure of CYP2C9 was reported by Wester et al. in 2004 [20], but no report is found about the crystal structure of CYP2C19. So, we need to build 3D structure model of CYP2C19 at first.

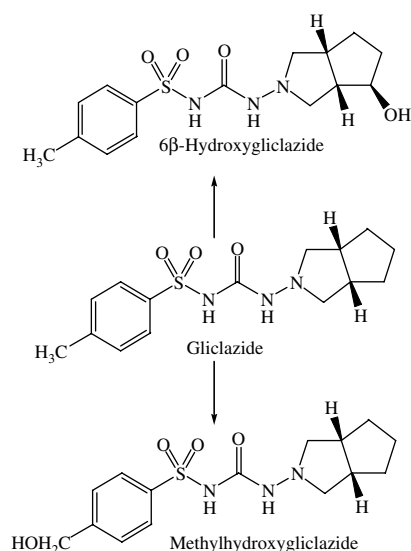


Fig. 1. The major metabolic pathways of glyclazide.

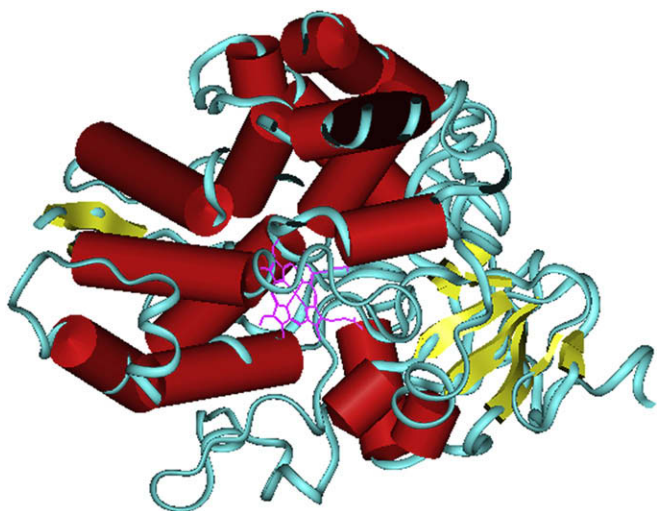


Fig. 2. The 3D structure of CYP2C19. Heme is represented by pink color, the  $\alpha$ -helix is represented by red color, the  $\beta$ -sheet is represented by yellow color. (For interpretation of the references to colour in this figure legend, the reader is referred to the web version of this article.)

### 3.1. 3D structure of CYP2C19

The initial 3D structure model of CYP2C19 was obtained by using homology method and the structural optimization was performed by using molecular mechanics and molecular dynamics simulations. After 500 ps of dynamics simulation, the equilibration was reached. The conformation with the lowest energy after the equilibration is chosen to be the final one and shown in Fig. 2. When measured by the Profile-3D method, the self-compatibility score is calculated to figure the compatibility of an amino acid sequence with the known 3D protein, and this is especially useful in the final phase of the protein structure modeling. The higher the score, the greater the compatibility between the structure and the amino acid sequence is. The self-compatibility score for CYP2C19 is 187, which is higher than the low score 96 and close to the top score 201. The PROCHECK program is used to check the stereochemical quality of a protein structure within the allowed Ramachandran region. The result is that 79% of residues in the 3D structure of CYP2C19 lie in the most favored regions, and only 0.09% of residues lie in disallowed regions of the Ramachandran plot. The results about Profile-3D and PROCHECK programs mean that 3D structure model of

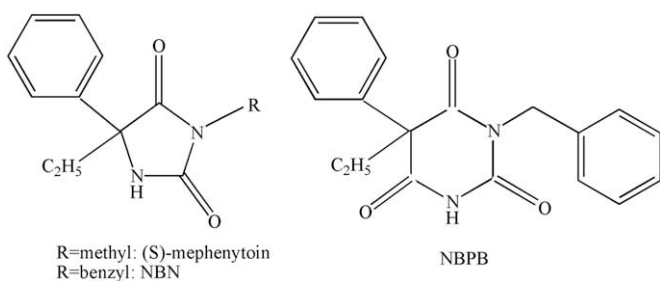


Fig. 3. Chemical structures of (S)-mephenytoin, N-3-benzyl-nirvanol (NBN) and N-3-benzyl-phenobarbital (NBPB).

Table 1  
The docking results of NBPB and NBN to CYP2C19

	Ludi score	$K_i$ value (theoretical) ( $\mu\text{M}$ )	$K_i$ value (experimental) ( $\mu\text{M}$ )
NBPB–CYP2C19	403	93	79
NBN–CYP2C19	363	231	250

The Ludi/InsightII module is used to calculate Ludi score; the theoretical  $K_i$  value is calculated by the relation between Ludi score and dissociation constant  $K_i$  (M). Ludi score =  $-100 \log K_i$ . The experimental  $K_i$  value is reported by Suzuki et al. [29].

CYP2C19 is very reasonable. In order to identify farther the reliability of the conformation of the active site in CYP2C19 model, the automated molecular docking was performed by using docking program InsightII/Affinity of the substrate (S)-mephenytoin, and the inhibitors (+)-N-3-benzyl-nirvanol (NBN), (–)-N-3-benzyl-phenobarbital (NBPB) (chemical structures of them are shown in Fig. 3) for CYP2C19. The active site of CYP2C19 has been reported by Oda et al. [29] and Lewis [30]. The docking result of (S)-mephenytoin indicates that (S)-mephenytoin is located near the heme iron and surrounded by some hydrophobic residues such as Val113, Ile205, Ala292, Ala297, Leu366, and Phe476. Phe476 and Ala297 are located nearby the phenyl ring of (S)-mephenytoin. These are consistent with the results of Tsao et al. [28] and Oda et al. [29]. The results of the inhibitors NBN and NBPB listed in Table 1 are in well agreement with the experimental results by Suzuki et al. [31]. So we think that the conformation of the active site in CYP2C19 model is reliable.

### 3.2. Docking of gliclazide to CYP2C9

The two CYP2C9–gliclazide complexes **1** and **2** were generated by using the InsightII/Affinity module and the structures are shown in Fig. 4. In both complexes,

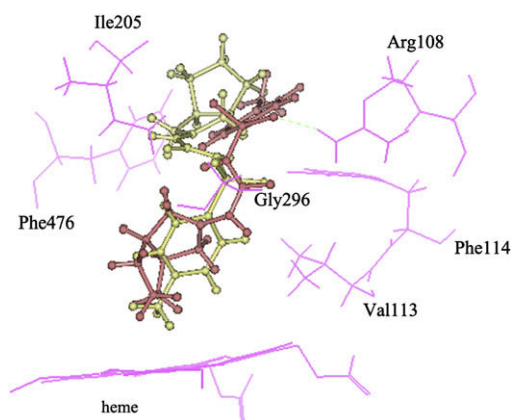


Fig. 4. An overlap of docking results of CYP2C9. Gliclazide in the CYP2C9–gliclazide complex **1** and **2** is represented by red and yellow color, respectively. In the CYP2C9–gliclazide complex **1**, one hydrogen bond is formed between gliclazide and Arg108, the bond distance is 2.11 Å and the bond angle is 164.41°. (For interpretation of the references to colour in this figure legend, the reader is referred to the web version of this article.)

Table 2

The total energy ( $E_{\text{total}}$ ), van der Waals energy ( $E_{\text{vdw}}$ ), and electrostatic energy ( $E_{\text{ele}}$ ) between gliclazide and individual residues in both CYP2C9–gliclazide complexes ( $E_{\text{total}} < -2.00$  kcal/mol)

Residue	$E_{\text{vdw}}$	$E_{\text{ele}}$	$E_{\text{total}}$
<i>CYP2C9–gliclazide complex 1</i>			
Enzyme	-42.02	-7.36	-49.38
Heme	-8.00	-1.46	-9.46
Phe114	-4.82	-1.21	-6.03
Gly296	-2.64	-2.90	-5.54
Arg108	-2.15	-1.32	-3.47
Val113	-2.83	-0.30	-3.13
Phe100	-3.08	0.50	-2.58
Asn204	-0.99	-1.49	-2.48
Ile205	-2.24	0.16	-2.08
Phe476	-1.98	-0.08	-2.06
<i>CYP2C9–gliclazide complex 2</i>			
Enzyme	-51.14	-5.53	-56.67
Heme	-9.40	-0.55	-9.95
Phe476	-4.51	-0.35	-4.86
Leu208	-3.30	-1.45	-4.75
Gly296	-2.52	-1.84	-4.36
Phe114	-4.18	-0.01	-4.19
Ile205	-2.62	-0.43	-3.05
Leu366	-3.03	0.25	-2.78
Val113	-1.84	-0.42	-2.26
Ala297	-2.17	0.13	-2.04

gliclazide is located in the center of the active site of CYP2C9. In the CYP2C9–gliclazide complex **1**, the distance from 6 $\beta$ -carbon atom to the heme is 4.33 Å which is suitable to form the 6 $\beta$ -hydroxygliclazide product [30]. A hydrogen bond formed between gliclazide and Arg108 in CYP2C9 is helpful for the stability of the CYP2C9–gliclazide complex **1**. In the CYP2C9–complex **2**, the distance from methyl-carbon to the heme is 3.89 Å which is suitable to form the methylhydroxygliclazide product [30]. There is no hydrogen bond formed between gliclazide and CYP2C9. From Table 2, one can see that the CYP2C9–gliclazide complex **2** is more stable because it has lower and more favorable total interaction energy of -56.67 kcal/mol than the CYP2C9–gliclazide complex **1** (-49.38 kcal/mol). The Ludi scores of both complexes are 396 and 464, respectively, which means that the affinity between gliclazide and CYP2C9 in the CYP2C9–gliclazide complex **2** is stronger than that in the CYP2C9–gliclazide complex **1**. The kinetic experimental results in Table 3 by part of the present authors is that  $K_m$  value of the CYP2C9–gliclazide complex **2** (methylhydroxygliclazide metabolic pathway) is 30.0  $\mu\text{M}$ , which is lower than 40.6  $\mu\text{M}$  of the CYP2C9–gliclazide complex **1** (6 $\beta$ -hydroxygliclazide metabolic pathway). The lower  $K_m$  value means stronger

affinity. Thus, the affinity of the CYP2C9–gliclazide complex **2** is stronger than that of the CYP2C9–gliclazide complex **1**. So our theoretical results about the affinity difference are in good agreement with the kinetic experimental results.

To determine the key residues in the two complexes, the interaction energies of gliclazide with each individual residue in the active site are calculated. Significant active-site residues in the models are identified by the total interaction energy. In general, the residues whose interaction energies with the ligand are lower than -1 kcal/mol are considered to be important in the complex. It is very convenient to discuss the results with this criterion. Herein, our criterion (-2 kcal/mol) is lower than -1 kcal/mol, which means the chosen residues are more important. The attractive electrostatic interaction or van der Waals interaction between heme and gliclazide is very important for binding orientation of gliclazide and absolutely necessary for the hydroxylation mechanism. From Table 2, one can see that heme, Val113, Phe114, Ile205, Gly296, and Phe476 have strong van der Waals and electrostatic interactions which are lower than -2 kcal/mol with gliclazide in the both complexes. So we think that they are the important anchoring residues for binding with gliclazide. Our theoretical results are in well agreement with the results by Melet et al. that Phe114 and Phe476 in CYP2C9 are important residues for the substrate binding and selectivity [32]. Hydrogen bond plays an important role for structure and function of biological molecules, especially for the enzyme catalytic reaction. In the CYP2C9–gliclazide complex **1**, Arg108 forms a hydrogen bond with gliclazide, this result indicates that Arg108 is also an important residue. This is consistent with the result by Ridderström et al. [33].

### 3.3. Docking of gliclazide to CYP2C19

The two CYP2C19–gliclazide complexes **1** and **2** were generated by using the InsightII/Affinity module as shown in Fig. 5. In both complexes, gliclazide is located in the center of the active site of CYP2C19. In the CYP2C19–gliclazide complex **1**, the distance from 6 $\beta$ -carbon atom to the heme is 5.27 Å which is suitable to form the 6 $\beta$ -hydroxygliclazide product [30]. A hydrogen bond formed between gliclazide and Asp293 in CYP2C19 is helpful for the stability of the CYP2C19–gliclazide complex **1**. In the CYP2C19–complex **2**, the distance from methyl-carbon to the heme is 4.05 Å which is suitable to form the methylhydroxygliclazide product [30]. There is a hydrogen bond formed between gliclazide and Arg97 in CYP2C19, which is helpful for the stability of the CYP2C19–gliclazide complex **2**. The Ludi scores of both

Table 3

Michaelis–Menten kinetic parameters of gliclazide hydroxylation

Species	6 $\beta$ -Hydroxygliclazide		Methylhydroxygliclazide	
	$K_m$	$V_{\text{max}}$	$K_m$	$V_{\text{max}}$
CYP2C9	40.6	0.6	30.0	0.6
CYP2C19	24.8	14.9	24.6	12.1

$V_{\text{max}}$  data shown are in units of picomoles per minute per picomole for rCYPs;  $K_m$  data shown are in units of microsomes. All data were means of duplicates.

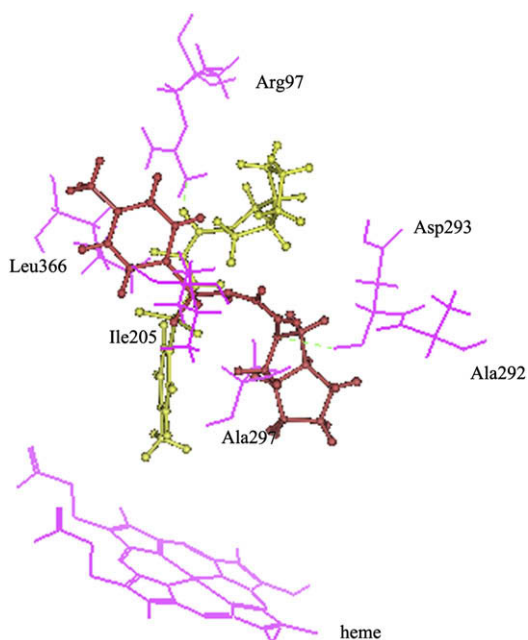


Fig. 5. An overlap of docking results of CYP2C19. Gliclazide in the CYP2C19–gliclazide complexes **1** and **2** is represented by red and yellow color, respectively. In the CYP2C19–gliclazide complex **1**, one hydrogen bond is formed between gliclazide and Glu300, the bond distance is 2.30 Å and the bond angle is 120.15°. In the CYP2C19–gliclazide complex **2**, one hydrogen bond is formed between gliclazide and Glu300, the bond distance is 2.39 Å and the bond angle is 145.48°. (For interpretation of the references to colour in this figure legend, the reader is referred to the web version of this article.)

complexes are 476 and 523, respectively, which mean higher affinity and stronger binding.

The results of the interaction energy are listed in Table 4. From Table 4, one can see that the CYP2C19–gliclazide complex **2** has lower and more favorable total interaction energy of –60.45 kcal/mol than the CYP2C19–gliclazide complex **1** (–54.12 kcal/mol). This means that the affinity between CYP2C19 and gliclazide in the CYP2C19–gliclazide complex **2** is stronger than that in the CYP2C19–gliclazide complex **1**, and this result is consistent with the kinetic experimental

Table 4

The total energy ( $E_{\text{total}}$ ), van der Waals energy ( $E_{\text{vdw}}$ ), and electrostatic energy ( $E_{\text{ele}}$ ) between gliclazide and individual residues in both CYP2C19–gliclazide complexes ( $E_{\text{total}} < -2.00$  kcal/mol)

Residue	$E_{\text{vdw}}$	$E_{\text{ele}}$	$E_{\text{total}}$
<i>CYP2C19–gliclazide complex 1</i>			
Enzyme	–49.70	–4.42	–54.12
Heme	–7.38	–2.35	–9.73
Glu300	–5.11	–1.90	–7.01
Leu366	–4.81	–0.59	–5.40
Ala297	–2.74	–1.16	–3.90
Val113	–2.01	–0.91	–2.92
Phe110	–2.50	–0.11	–2.61
Thr301	–3.24	0.80	–2.44
Phe428	–2.12	–0.30	–2.42
Ile362	–2.36	–0.05	–2.41
Thr299	–1.12	–1.28	–2.40
<i>CYP2C19–gliclazide complex 2</i>			
Enzyme	–59.48	–0.97	–60.45
Glu300	–4.35	–1.66	–6.01
Heme	–4.24	–1.35	–5.59
Arg433	–4.90	0.38	–4.52
Thr301	–2.52	–1.84	–4.36
Leu366	–4.47	0.28	–4.19
Ile205	–3.62	–0.39	–4.01
Phe428	–2.90	–0.28	–3.18
Ile362	–3.16	0.17	–2.99
Ala297	–3.42	0.44	–2.98
Val436	–2.20	–0.18	–2.38
Phe476	–2.43	0.19	–2.24
Arg124	–2.06	–0.16	–2.22
Ser429	–2.40	0.40	–2.00

results shown in Table 3 by part of the present authors. To determine the key residues in the two complexes, the interaction energies of gliclazide with each individual residue in the active site are calculated. From Table 4, one can see that heme, Arg97, Val113, Ile205, Ala292, Asp293, Ala297, and Leu366 have strong van der Waals and electrostatic interactions which are lower than –2 kcal/mol with gliclazide in the both complexes. So we think that they are the important anchoring residues for binding with gliclazide. Especially, Arg97 and Asp293 form hydrogen bonds with gliclazide in complexes **1**

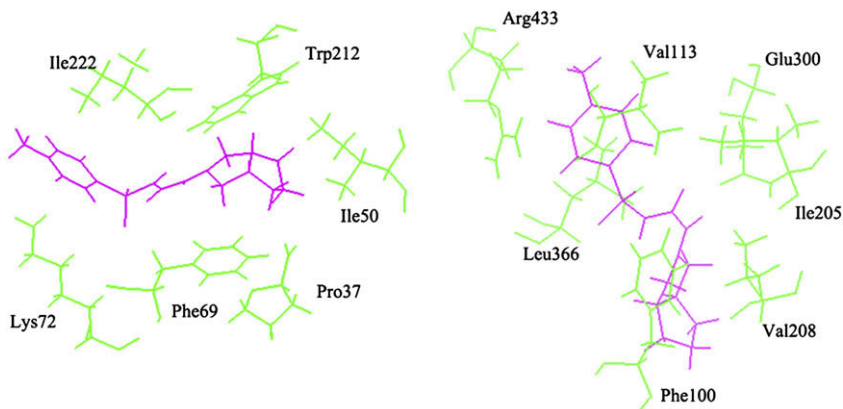


Fig. 6. Overlaps of the dockings of gliclazide to the second binding sites in CYP2C9 and CYP2C19. The CYP2C9–gliclazide complex **3** is at left and the CYP2C19–gliclazide complex **3** is at right.

Table 5  
The changes of the affinity between gliclazide with two enzymes by substrate inhibition

		6 $\beta$ -Hydroxygliclazide		Methylhydroxygliclazide	
		The total interaction energy	Ludi score	The total interaction energy	Ludi score
CYP2C9	No substrate inhibition	-49.38	396	-56.67	464
	Substrate inhibition	-38.56	365	-41.26	387
CYP2C19	No substrate inhibition	-54.12	476	-60.45	523
	Substrate inhibition	-41.50	424	-44.45	447

and **2**, respectively, so that they play an important role for the stability of the complexes. Our results about Asp293 and Ala297 are consistent with the results of Oda et al. [29].

### 3.4. Substrate inhibition

Substrate inhibition is an atypical kinetic phenomenon which is often observed in vitro [34–37]. The mechanism of substrate inhibition has been explained clearly [38,39] that there are two substrate binding sites in enzyme, one site is productive and the other site is inhibitory and operable at

high substrate concentrations, which results in decreased velocity with increasing concentrations.

With the aid of the binding-site module/InsightII [40], we succeeded in finding the second binding site in CYP2C19 which is near the active site of gliclazide. Using Affinity module, gliclazide is docked into the second binding site of CYP2C19 and this docking complex (denoted as CYP2C19–gliclazide complex **3**) is shown in Fig. 6. The van der Waals, the electrostatic interaction, and the total interaction energies in CYP2C19–gliclazide complex **3** are -11.33, -10.39, and -21.72 kcal/mol, respectively, and the total interaction energy in CYP2C19–gliclazide complex **3** is the highest in three CYP2C19–gliclazide complexes. Thus, the Affinity program was performed to dock gliclazide to the active site in CYP2C19–gliclazide complex **3** while gliclazide in the second binding site was merged to CYP2C19. Then two docking complexes, corresponding to two metabolic pathways, were generated. The total interaction energies and Ludi scores of two docking complexes are listed in Table 5. From Table 5, one can see the predominant decreases of the total interaction energies and Ludi scores because of the binding of gliclazide in the binding site. The changes of the affinity between gliclazide and CYP2C19 confirm convincingly that there is substrate inhibition in metabolism of CYP2C19 for gliclazide. The similar result has also been found in metabolism of CYP2C9 for gliclazide and the obtained CYP2C9–gliclazide complex **3** is shown in Fig. 6 and Table 5, too. The experimental results in Fig. 7 indicate that both the catalytic reactions' velocities increase with the increasing

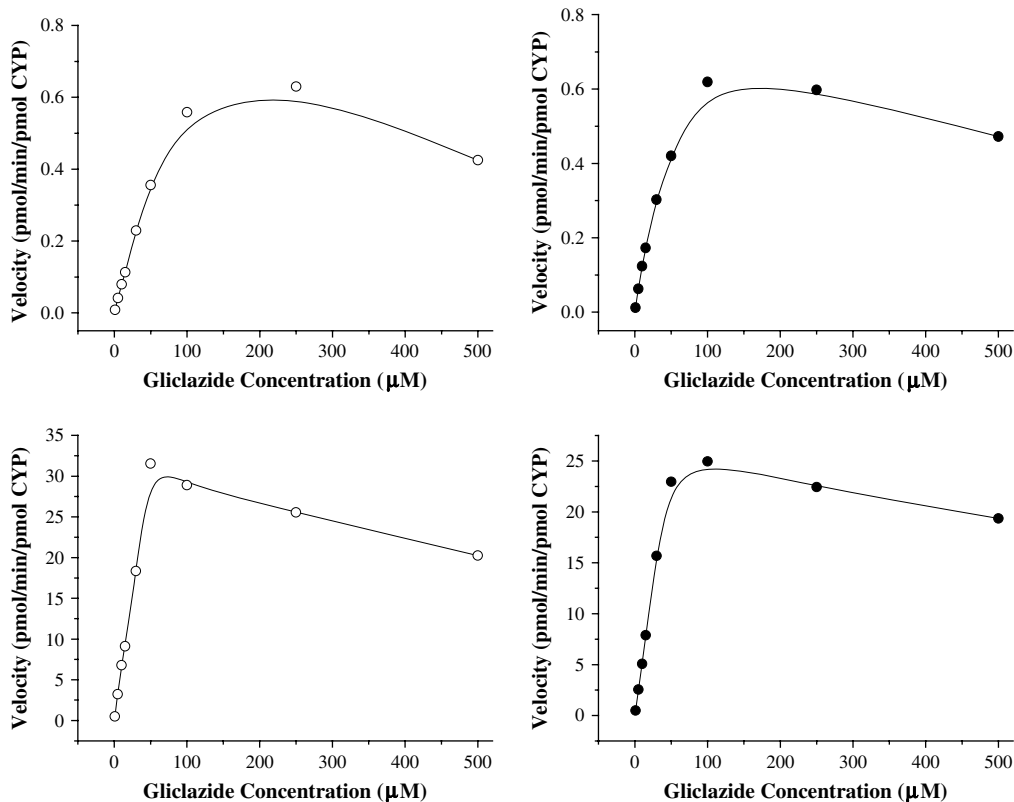


Fig. 7. Enzymatic kinetic modeling of 6 $\beta$ -hydroxygliclazide formation (open plot) and methylhydroxygliclazide formation (closed plot) in recombinant CYP2C9 (up) and CYP2C19 (down). Results are presented as the mean of duplicates.

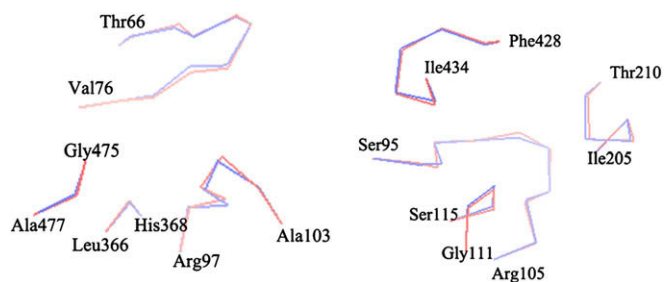


Fig. 8. Overlaps of the conformational changes of CYP2C9 and CYP2C19 by substrate inhibition. CYP2C9 is at left and CYP2C19 is at right.

concentration of gliclazide. However, when gliclazide is up to about 200 and 100  $\mu\text{M}$  for CYP2C9 and CYP2C19, respectively, the velocities begin to decrease obviously. This is substrate inhibition obviously. So, our theoretical results about substrate inhibition are in good agreement with the experimental results in quality.

In order to investigate the mechanism of the changes of the affinity, we compared the structures of CYP2C19 and CYP2C19–gliclazide complex **3**. All  $\text{C}\alpha$  of the whole enzymes were used, however, the conformational change between CYP2C19 and CYP2C19–gliclazide complex **3** only exists in the active site because of the key feature of the flexible docking mentioned in Section 2. The RMSD of the active sites in CYP2C19 and CYP2C19–gliclazide complex **3** is 2.26 Å. The major conformational changes of the active sites in CYP2C19 and CYP2C19–gliclazide complex **3** are shown in Fig. 8. One can see that the docking of gliclazide in the second binding site causes the conformational changes of residues Ser95–Arg105, Gly111–Ser115, Ile205–Thr210, and Phe428–Ile434. Especially, Val113, Ile205, Phe428, Ser429, and Arg433 are suggested to be the important residues in CYP2C19 for binding with gliclazide as seen from Table 4. So we think that the conformational change is major reason to a decrease in the affinity. The substrate inhibition of CYP2C9 employs the same mechanism as CYP2C19 and the conformational changes in CYP2C9 are shown in Fig. 8, too.

#### 4. Conclusion

In the present paper, with homology modeling techniques, molecular mechanics, and molecular dynamics methods, a reliable and reasonable 3D structure of CYP2C19 was built. In order to check further the reliability of the 3D structure of CYP2C19, the automated molecular docking was performed by using docking program Affinity of the substrate (*S*)-mephenytoin, and the inhibitors (+)-*N*-3-benzyl-nirvanol (NBN) and (–)-*N*-3-benzyl-phenobarbital (NBPB) for CYP2C19. Our docking results are consistent with the reported results.

With the aid of the automatic molecular docking, the metabolic effects of CYP2C9 and CYP2C19 for gliclazide in two different pathways were studied by InsightII/Affinity program. The affinity of both enzymes and gliclazide in methylhydroxylgliclazide pathway is stronger than the one

in 6 $\beta$ -hydroxygliclazide pathway because the interaction energies in methylhydroxylgliclazide pathway are lower than in 6 $\beta$ -hydroxylation pathway, and Ludi score for both enzymes in methylhydroxylation pathway are all higher than those in 6 $\beta$ -hydroxylation pathway. Then we identify that heme, Val113, Phe114, Ile205, Gly296, and Phe476 of CYP2C9, heme, Arg97, Val113, Ile205, Ala292, Asp293, Ala297, and Leu366 of CYP2C19 are the most important anchoring residues for binding with gliclazide. It is notable that there are significant substrate inhibition phenomena in metabolisms of CYP2C9 and CYP2C19 for gliclazide. Both enzymes employ the same mechanism that the bindings of gliclazide near the active sites can change the conformation of the active site and decrease efficiently the affinity between gliclazide in the active site and enzymes in both metabolic pathways. Our results are consistent with the kinetic experimental results. We hope that our results are helpful for the future research of gliclazide metabolism.

#### Acknowledgement

This work is supported by the National Science Foundation of China (20333050, 20673044), Doctor Foundation by the Ministry of Education, Foundation for University Key Teacher by the Ministry of Education, Key subject of Science and Technology by the Ministry of Education of China, and Key subject of Science and Technology by Jilin Province.

#### References

- [1] D.K.G. Andersson, K. Svardsudd, *Diabetes Care* 18 (1995) 1534.
- [2] J.F. Yale, *J. Am. Soc. Nephrol.* 16 (2005) S7.
- [3] H.E. Lebovitz, *Med. Clin. North Am.* 88 (2004) 847.
- [4] G.-P. Zhong, H.-C. Bi, S.-F. Zhou, X. Chen, M. Huang, *J. Mass Spectrom.* 40 (2005) 1462–1471.
- [5] P. Zimmet, K.G. Alberti, J. Shaw, *Nature* 414 (2001) 782–787.
- [6] D.E. James, *J. Clin. Invest.* 115 (2005) 219–221.
- [7] M.O. Goodarzi, M. Bryer-Ash, *Diabetes Obes. Metab.* 7 (2005) 654–665.
- [8] S. Ristic, C. Collober-Maugeais, E. Pecher, F. Cressier, *Diabet. Med.* 23 (2006) 757–762.
- [9] A.J. Ward, M. Salas, J.J. Caro, D. Owens, *Cost Eff. Resour. Alloc.* 2 (2004) 2–10.
- [10] K.J. Palmer, R.N. Brogden, *Drugs* 46 (1993) 92.
- [11] A.J. Krentz, C.J. Bailey, *Drugs* 65 (2005) 385.
- [12] A.J. Garber, *Diabetes Obes. Metab.* 2 (2000) 139–147.
- [13] U. Lindblad, A. Melander, *Diabetes Obes. Metab.* 2 (2000) 25–31.
- [14] T. Oida, K. Yoshida, A. Kagemoto, *Xenobiotica* 15 (1985) 87–96.
- [15] A.R. Taylor, R.D. Brownsill, H. Grandon, *Drug Metab. Dispos.* 24 (1996) 55–64.
- [16] J.Y. Park, K.A. Kim, P.W. Park, *Clin. Pharmacol. Ther.* 74 (2003) 334–340.
- [17] Y.-F. Zhang, D.-Y. Si, X.-Y. Chen, N. Lin, Y.J. Guo, H. Zhou, D.-F. Zhong, *Br. J. Clin. Pharmacol.* 64 (2007) 67–74.
- [18] InsightII, Version 98.0, Accelrys Inc., San Diego, USA, 1998.
- [19] Homology User Guide, Accelrys Inc., San Diego, USA, 1999.
- [20] M.R. Wester, J.K. Yano, G.A. Schoch, C. Yang, K.J. Griffin, C. David Stout, E.F. Johnson, *J. Biol. Chem.* 279 (2004) 35630–35637.
- [21] H. Suzuki, M. Byron Kneller, D.A. Rock, J.P. Jones, W.F. Trager, A.E. Rettie, *Arch. Biochem. Biophys.* 429 (2004) 1–15.
- [22] Discover3 User Guide, Accelrys Inc., San Diego, USA, 1999.
- [23] Profile-3D User Guide, Accelrys Inc., San Diego, USA, 1999.

- [24] R.A. Laskowski, M.W. MacArthur, D.S. Moss, J.M. Thornton, J. Appl. Crystallogr. 26 (1993) 283–291.
- [25] Affinity User Guide, Accelrys Inc., San Diego, USA, 1999.
- [26] D.R. Nelson, L. Koymans, T. Kamataki, J.J. Stegeman, R. Feyereisen, D.J. Waxman, M.R. Waterman, O. Gotoh, M.J. Coon, R.W. Estabrook, Pharmacogenetics 6 (1996) 1–42.
- [27] F.P. Guengerich, Chem. Res. Toxicol. 14 (2001) 611–650.
- [28] C.C. Tsao, M.R. Wester, B. Ghanayem, S.J. Coulter, B. Chanas, E.F. Johnson, J.A. Goldstein, Biochemistry 40 (2001) 1937–1944.
- [29] A. Oda, N. Yamaotsu, S. Hirono, Pharm. Res. 21 (2004) 2270–2278.
- [30] D.F.V. Lewis, Arch. Biochem. Biophys. 409 (2003) 32–44.
- [31] H. Suzuki, M. Byron Kneller, R.L. Haining, W.F. Trager, A.E. Rettie, Drug Metab. Dispos. 30 (2002) 235–239.
- [32] A. Melet, N. Assrir, P. Jean, M. Pilar Lopez-Garcia, C. Arques-Soares, M. Jaouen, P.M. Dansette, M.A. Sari, D. Mansuy, Arch. Biochem. Biophys. 409 (2003) 80–91.
- [33] M. Ridderström, C. Masimirembwa, S. Trump-Kallmeyer, M. Ahlefeldt, C. Otter, T.B. Andersson, Biochem. Biophys. Res. Commun. 270 (2000) 983–987.
- [34] C.-Y. Tang, M. Shou, Q. Mei, J. Pharmacol. Exp. Ther. 293 (2000) 453.
- [35] J. Zhao, T. Leemann, P. Ayer, Life Sci. 51 (1992) 575–581.
- [36] T.S. Tracy, J.M. Hutzler, R.L. Haining, Drug Metab. Dispos. 30 (2002) 385–390.
- [37] Y. Lin, P. Lu, C. Tang, Drug Metab. Dispos. 29 (2001) 368–374.
- [38] M. Shou, Y. Lin, P. Lu, Curr. Drug. Metab. 2 (2001) 17–36.
- [39] J.M. Hutzler, T.S. Tracy, Drug Metab. Dispos. 30 (2002) 355–362.
- [40] Binding Site Analysis User Guide, Accelrys Inc., San Diego, USA, 1999.